STATISTICAL PROPERTIES OF COMPOSITE DISTORTIONS IN HFC SYSTEMS AND THEIR EFFECTS ON DIGITAL CHANNELS

By Dr. Ron D. Katznelson, CTO
Broadband Innovations, Inc., San Diego CA

ABSTRACT

The statistical properties of CTB and CSO distortion terms associated with the analog channels carried on Hybrid Fiber Coax (HFC) are presented. Both simulation and measurement results show that these distortion components falling on individual channels have amplitude Probability Density Function that is nearly Rayleigh distributed (having a Standard Deviation of 5.7 dB). It is shown that both CTB and CSO components have significant likelihood of having peak envelope power fluctuations that exceed their average (measured) power levels by more than 15 dB. The temporal statistical properties of these distortion components are also examined and evidence for peak envelope power fluctuations with characteristic times on the order of 100 microseconds is presented. The implications of these statistical properties for 256 QAM digital downstream channels on which such CTB and CSO components fall are discussed. It is shown that some currently prevailing link budget design practices do not provide sufficient margin for reliable 256 QAM operation, particularly in systems that are rich with Narrowcast combining of digital channels such as cable modem and Video on Demand (VOD) applications. Several mitigation strategies and improved design practices are subsequently reviewed. These involve physical layer choices for longer digital interleaver depth, establishing QAM frequency offset relative to the analog channel grid, improved CTB and CSO specifications for cable modems and digital set-top tuners and tighter aggregate noise floor specifications for head-end RF transmission gear.

1 Introduction

Nonlinear distortions and limited dynamic range in multichannel carrier systems has received renewed attention with the proliferation of digital devices and the industry's move to launch 256 QAM digital services. Now, composite distortion components often become the bottleneck that it never was for the predominant 64 QAM service. Although the installed base of digital subscriber set-tops and cable modems is predominantly 256 QAM capable, many cable operators have yet to migrate to 256 QAM transmissions successfully. As it turns out, the 256 QAM's whopping 44% increase in channel information payload capacity over that of 64 QAM comes at a considerable cost in noise and interference margin requirements. Operating reliable 256 QAM downstream links is more challenging due to the factors described in Section 5. Suffice it to say here that as a result of the cumulative effect of these factors, the noise margin left for further noise degradations in 256 QAM all but disappears [1].

2 Composite Distortions Effect on Digital Channels

Composite Triple Beats (CTB) and Composite Second Order (CSO) distortion components produced by intermodulation of analog TV carriers can become the dominant degrading factor for digital cable QAM channels [1],[2],[3],[4],[5]. It is generally accepted that in thermal noise environments, a Carrier to Noise Ratio (*C/N*) of 30-35 dB provides adequate operating margins for 256 QAM [6]. It is also generally known that cable systems normally operate with CTB or CSO levels that

meet or exceed a Carrier-to-Interference (*C/I*) ratio of 53 dB, as required in Reference [6]. These levels correspond to a *C/I* of 47 dB for a QAM signal carried with levels that are 6 dB below the analog carriers. The question that may arise is *why should distortion components having average power levels that are 12-15 dB below the noise level have any appreciable degradation effects on the QAM channel performance?* The short answer is that the average envelope power of composite distortion terms (which is what one observes in a spectrum analyzer measurement) is deceptively low in comparison to its occasional peak envelope power.

3 Description of Composite Distortion Terms

In a multicarrier CATV system one often represents the signal to be communicated as

$$\textbf{(1)} \qquad S(t) = \sum_{n=1}^{N} A_n \cos\left(\omega_n t + \theta_n\right),$$

where A_n, ω_n and θ_n are the amplitude, the angular frequency and phase of the nth carrier signal. We shall have occasion to investigate the unmodulated case, $A_n = A$ for all n and the modulated case, where the modulations in A_n are sufficiently slow compared to the essential RF period of $S(t)$ so as to treat them as constants (or as random variables) during such RF period discussed below. This assumption is justified since statistically, the baseband video modulation power spectrum has negligible energy at 6 MHz or 1.25 MHz, which are possible nominal periodicities of the RF signal. Furthermore, for television signals, we shall assume that other subcarriers such as the single sided audio and chroma subcarriers associated with each television carrier are sufficiently low in amplitude in comparison with the visual carrier so as to treat them as a separate additive noise process. The above assumptions permit us to treat Equation (1) as a reasonable representation of the signal in our problem.

Upon subjecting $S(t)$ to a memoryless nonlinear distortion device having a transfer function given by $y = x + \alpha x^2 + \beta x^3$, where x is the input voltage and y the output voltage, we obtain intermodulation products of second and third order and in this work we have assumed no higher order distortion exist in the nonlinear transfer function. The type and relative amplitudes of the intermodulation components that are so obtained are well known and are tabulated elsewhere [7]. We shall be interested in components of the following form:

(1-A) Second-Order

$$\frac{1}{2}\alpha A_n A_k \cos[(\omega_n \pm \omega_k)t + \theta_n \pm \theta_k]$$

(1-B) Third-Order

$$\frac{1}{4}\beta A_n A_k A_m \cos[(\omega_n \pm \omega_k \pm \omega_m)t + \theta_n \pm \theta_k \pm \theta_m]$$

wherein for a frequency plan in which virtually all carriers are nominally 6 MHz apart, many distortion components fall on the same nominal frequency. The way these terms combine and the amplitude excursions of the resultant composite waveform falling on each channel depend on the number of carriers N, the specific arrangement of the amplitudes, the frequencies and the phases (A_n, ω_n and θ_n). It is important to note that even in the simplest case in which we assume no modulation (i.e. $A_n = A$ for all n), a particular choice of the remaining parameters may submit to a solution that will not apply to any other combination. Furthermore, the exact values of these parameters may never be known for any particular head-end. Of particular significance may be identifying any frequency combinations that may yield coherent combining (for which $\omega_p = \omega_n \pm \omega_k \pm \omega_m$, for example) and taking account of the special results it entails.

Moreover, if the whole set of channels is coherent and locked to a comb (IRC or HRC), then one would need to specify only each of the phase values θ_n and the result will be specific to that phase constellation but not necessarily to any other[1]. It now becomes clear that countless combinations would have to be considered as special cases and the usefulness of any of them for making general statements is at best doubtful.

An alternative approach we adopt here is to make the (realistic) assumption that all the frequencies ω_n are linearly independent over the rational field, or stated another way, that there exists no set of integers Q_n's (positive, zero or negative) such that

$$\sum_{n=1}^{N} Q_n \omega_n = 0 .$$

It is only under such an assumption that one may obtain results that apply across many different frequency realizations within the tolerance of the nominal frequency plan. For each such realization (a given collection of ω_n and θ_n) in our model, an *unmodulated* signal $S(t)$ of Equation (1) is deterministic and nothing about it is random. Because the precise frequencies are assumed to be linearly independent, the period of the signal $S(t)$ is infinite. Consequently, the period of any of its distortion components is also infinite. With this assumption, it is mathematically possible to show that a characterization of *any* feature, measure, frequency of occurrence or distribution over a long enough observation period T from t_0 to t_0+T, would be repeatable regardless of when t_0 is. This, in general, cannot be assured for choices of exact frequencies that are linearly dependent over the rational field.

[1] In fact, there are very atypical (but deliberate) phase constellations that yield very low distortion values that are otherwise extremely unlikely to be found at random. A method to arrive at such constellations is described in [8].

We note that, strictly speaking, the nominal frequencies of the Standard CATV channel plan are a linearly dependent set of frequency values. However, in non-coherent headends, their actual values are given by[2]

$$\begin{aligned} \omega_n &= (n+8)\cdot\omega_C + \omega_0 + \Delta\omega_n \\ &= 2\pi\,[(n+8) f_C + f_0 + \Delta f_n] \end{aligned} \qquad (2)$$

where f_C = 6 MHz, f_0 =1.25 MHz (the visual carrier offset from the channel edge) and Δf_n is the individual actual deviation from the nominal frequency due to tolerance. These deviations can be on the order of a few hundred Hz to a few kHz, and are the basis and justification for the assumption we make about their linear independence over the rationales[3]. When one uses the values in Equation (2) for the frequencies one obtains composite distortion frequencies that have linear combinations of the deviation values. For example, third order components falling on frequencies $\omega_n + \omega_k - \omega_m$ have frequency values of $p\omega_C + \omega_0 + \Delta\omega_n + \Delta\omega_k - \Delta\omega_m$ with p an integer designating the channel. Similarly second order terms falling on frequencies $\omega_n + \omega_k$ have frequency values of $q\omega_C + 2\omega_0 + \Delta\omega_n + \Delta\omega_k$ with q another channel designating integer. Because the deviation frequencies $\Delta\omega_n$ are linearly

[2] We are ignoring the special case of Channels 5 and 6 that are offset by 2 MHz. Throughout this study, these channels and all others up to and including A4 were omitted, i.e. A_n=0 for n=4 through n=9 in Equations (1) and (2) above. The last channel in the array was at n=81, making up a total of 75 carriers.

[3] Because there is no relationship between the deviations Δf_n for each channel in a non-coherent system, these values can be thought of as drawn at random from the real line near the origin. Because the rationals form a set of measure zero on the real line, the probability that any random pair of numbers Δf_n and Δf_k drawn from the real line are linearly dependent over the rationals (i.e. that $\Delta f_n / \Delta f_k$ is rational) is zero.

independent over the rationales for all values of *n,* we conclude that *all possible beat frequencies produced by any combination of such deviation terms must all be distinct frequencies*.

The observation above provides certain clarity and resolution to predictions of the average power levels of composite distortion terms, as there are no terms that can combine coherently. In this case, counting the number of composite terms on any given frequency range would yield the exact power level of such components. Thus, precise derivations for such numbers [9] or tight approximations [10] can be very useful and the theoretical prediction of the average power in the unmodulated case is therefore straightforward. It is other characteristics of the composite distortion terms such as the envelope fluctuations and their temporal behavior that are of great interest. To that end, this author has embarked on a theoretical study comprising an analytical effort [11] and an empirical simulation effort, parts of which are reported in the next sections.

4 Mathematical Background and the Simulation Approach

By rewriting Equation (1) using the defined frequencies of Equation (2) we find that the simulation problem at hand is that of forming representations of, and operations with, $S(t)$ given by:

(3)

$$S(t) = \\ = \sum_{n=1}^{N} A_n \cos\{[(n+8)\cdot\omega_C + \omega_0]t + \Delta\omega_n t + \theta_n\}$$

wherein we have grouped separately the frequency terms that correspond to the (linearly dependent) nominal frequencies. In studying the distortion components we would need to select the frequencies and apply the expression for $S(t)$ from Equation (3) into the nonlinear transfer function $y = x + \alpha x^2 + \beta x^3$ by setting $x = S(t)$ and process the results to obtain a measure of interest that is representative on average over the observation time interval. If, for example, we wish to study a composite second order frequency-addition beat of the form given in Equation (1-A) above we would have a collection of like-frequency terms that fall on the sum-frequency of interest designated by the frequency index p:

(3-A)

$$y_{CSO}(p) = \\ = \sum_n A_n A_{p-n} \cos[(\omega_n + \omega_{p-n})t + \theta_n + \theta_{p-n}] = \\ = \sum_n A_n A_{p-n} \cos[(p\omega_C + 2\omega_0 + \Delta\omega_n + \Delta\omega_{p-n})t + \theta_n + \theta_{p-n}]$$

These terms form a narrow band signal about the frequency $p\omega_C + 2\omega_0$ with an envelope function given by

(3-B)

$$\mathrm{Env}[y_{CSO}(p),(t)] = \\ = \sum_n \sum_m A_n A_{p-n} A_m A_{p-m} \times \\ \times \cos[(\Delta\omega_n + \Delta\omega_{p-n} - \Delta\omega_m - \Delta\omega_{p-m})t + \\ + \theta_n + \theta_{p-n} - \theta_m - \theta_{p-m}]$$

where the meaning of a signal's envelope is that ascribed to it in the classic treatise by Dugundji [12]. In this work we are focusing on the statistical characteristics of the envelope (amplitudes) of these composite distortion terms rather than their RF statistics because it is more closely related to the demodulated baseband disturbances that affect BER performance of digital set-tops and cable modems. When we analyze such envelope terms, we obtain functions that depend on the amplitudes, the deviation frequencies and phases $\Delta\omega_n, \theta_n$, but not explicitly on the actual frequencies. Thus, for a given signal $S(t)$ and a given set of amplitudes, forming a statistical measure over time associated with such envelope terms essentially amounts to

time-averaging of some (nonlinear) function $F_S(\Delta\omega_n t, \theta_n; n=1 \text{ to } N)$. That function might be the envelope's value occurrence rate or joint correlation products of envelope values, etc. The function $F_S(\bullet)$ is representative of the kind of processing, data collection and classification that would be used. Fortunately, the assumption that the frequencies of $S(t)$ are linearly independent provides a powerful tool to simplify the simulations of these time-averages. It is based on a fundamental theorem in Ergodic Theory known as the Kronecker-Weyl theorem [13]:

4.1 Kronecker-Weyl Theorem.

The Kronecker-Weyl (K-W) theorem for multiply periodic functions $F(\psi_1, \psi_2, \cdots, \psi_N) \equiv F(\mathbf{\Psi})$ defined on the N dimensional torus, on which each of the ψ_j ranges from 0 to 2π and on which $F(\mathbf{\Psi}') = F(\mathbf{\Psi}'')$ if $\psi_j' = \psi_j''$ (modulo 2π) for all j, states the following:
If

(4) $$\psi_j = \Omega_j t + \theta_j$$

and if the frequencies Ω_j are linearly independent over the rational field, then

(5)
$$\frac{1}{T}\int_0^T F[\mathbf{\Psi}(t)]dt \quad \rightarrow$$
$$\rightarrow \frac{1}{(2\pi)^N}\int_0^{2\pi}\cdots\int_0^{2\pi} F(\psi_1, \psi_2, \cdots, \psi_N)\, d\psi_1 d\psi_2 \cdots d\psi_N$$
as $T \rightarrow \infty$
.

Stated another way, under the conditions that satisfy the K-W theorem, we can avoid having to select the frequency deviations $\Delta\omega_j$ and replace time averages by averages over all the phases. In reference to the CSO envelope term expressed above (as also applies for CTB or other distortion terms), for our simulations, we identify Ω_j of the K-W theorem with $\Delta\omega_j$ and by using Equation (4) we rewrite Equation (3):

(6)
$$S(t) = \sum_{n=1}^{N} A_n \cos\{[(n+8)\cdot\omega_C + \omega_0]t + \psi_n\}$$

In our computer simulations we thus form an ensemble of uniformly distributed random phase vectors $\mathbf{\Psi} \equiv (\psi_1, \psi_2, \cdots, \psi_N)$ with independent components on the N dimensional torus. For each such randomly drawn phase vector we compute $S(t)$ in accordance with Equation (6) and obtain a function of t that becomes a member of the analysis ensemble. Since we have selected the Standard frequency plan, the period of every $S(t)$ of the ensemble is 1.25 MHz and after appropriate model distortions are introduced, an FFT routine is employed to obtain envelopes of composite distortion terms on specific frequencies. It should be noted that the dependence on time remaining in $S(t)$ of Equation (6) is used only to obtain the spectral components of interest, and not for time averaging.

4.2 Modulation Statistics Assumed

In addition to simulations of the CW case, we simulated independent modulations on each of the carriers. Because in these simulations, we were focused only on first-order statistics (i.e. amplitude distributions and joint densities), time correlation effects (i.e. second-order statistics) associated with the analog video signals were not needed and only first-order statistics of the amplitudes were used. These distributions were computationally constructed from first-order statistics of NTSC luminance values, as they control the amplitude of the visual carrier. NTSC Luminance distribution values were taken from the work done by Philips researchers [14] in their work that led to the PAL system.

Appropriate account was made for blanking (75% level) and synch (100% level) periods and the resultant distribution is shown in Figure 1. Effects of amplitude modulation were simulated by forming the ensemble of functions of Equation (6) by the use of an expanded ensemble of random variables including the amplitudes, $\{\psi_1, \psi_2, \cdots, \psi_N, A_1, A_2, \cdots, A_N\}$, where the phases are drawn independently from a uniform distribution over [0, 2π] and the amplitudes are drawn independently from the distribution in Figure 1. That way, an ensemble of millions of realizations of $S(t)$, and consequently all related CSO and CTB distortion terms on every channel, was computed and analyzed. The results for the modulated and the unmodulated cases are shown in subsequent sections.

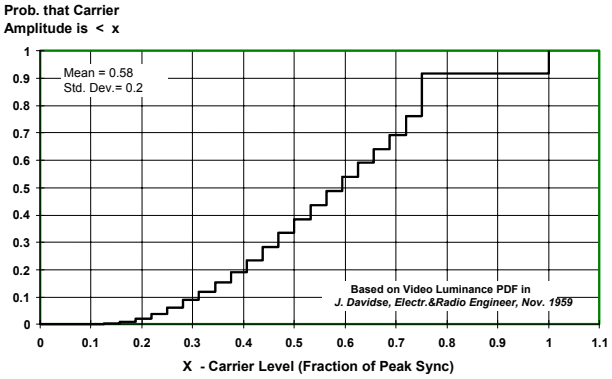

Figure 1. Cumulative probability density of RF amplitudes of a video modulated NTSC television signal. This function was used for simulating the independent modulation of 75 carriers. The function was constructed based on video luminance distributions provided in Reference [14].

4.3 Composite Distortions – Simulation Results and Discussion

4.3.1 Amplitude Statistics of Composite Distortions

Very few studies were found related to the probability density functions of CTB/CSO distortion components. One histogram was reported for a CW HRC system [15], although it was not clear what the source of phase fluctuations was. A more comprehensive landmark study involving real headend in a controlled laboratory was reported in Reference [4]. Both our simulations and the above referenced measurement results show that these distortion components falling on individual channels have amplitude Probability Density Functions (PDF) that are nearly Rayleigh. The Rayleigh probability density function is given by [16]:

$$f(x) = \frac{x}{a^2}\exp\left(\frac{x^2}{2a^2}\right)$$

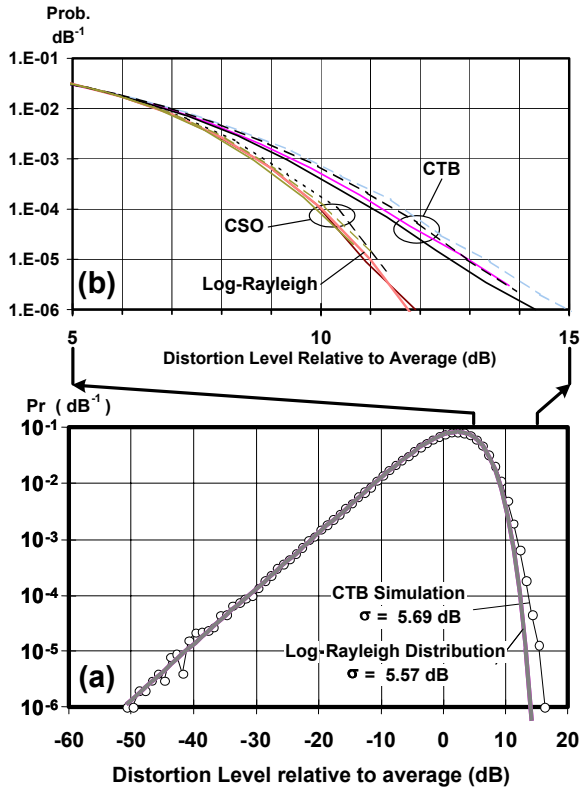

Figure 2. Probability density function of the amplitude of simulated CTB and CSO terms due to third order and second order distortions in a CATV system using the Standard Frequency plan with 75 analog video modulated carriers. On the ordinate, the amplitude squared is expressed in dB relative to the average envelope value and the corresponding probability per dB is plotted in the co-ordinate. For comparison, a Rayleigh density transformed to the dB scale (thus called Log-Rayleigh) is also shown in solid line. An expanded view from 5 to 15 dB is provided in (b), where curves for the CW case and the modulated case are shown with solid lines and broken lines respectively.

Figure 2a shows the simulation results for the probability density function of the amplitude of a simulated CTB term due to third order distortion in a CATV system employing the Standard Frequency plan with 75 analog video modulated carriers. For comparison, a Rayleigh density transformed to the dB scale (thus called Log-Rayleigh) is also shown. The Rayleigh density is relevant in this comparison because it describes the envelope probability density of a Gaussian process, which is the limit case for a linear combination of a large number of arbitrarily distributed, statistically independent random processes. One would expect that because the CTB and CSO terms encountered in CATV are comprised respectively from thousands and hundreds of beat components, the Rayleigh limit would be nearly approached. However, while there appears to be a good match at lower amplitude levels, relevant deviations at large relative amplitudes are seen for CTB in Figure 2b. This slight deviation is due to the statistical dependence among these thousands of components. It is argued that, in this case, because there are only $2\times75 = 150$ *independent degrees of freedom* (random phase and amplitude of each of the 75 carriers) affecting the phase and amplitude values of the individual *thousands* of beat components, these must be statistically dependent. Because the number of components in the CSO term is of the order of less than 100, these component values depend less on common degrees of freedom and are less correlated. The degree and differences of the correlations for CSO and CTB terms and their respective effects on envelope statistics are further addressed in [11].

Noteworthy is the observation that as one inspects distortion terms on different channels, the absolute levels of the envelopes differ, but when normalized to their respective average envelope power, the PDFs of the CTB and CSO components on every channel essentially follow closely the results for the CTB term shown in Figure 2(a). Moreover, each of these distributions, like the Rayleigh distribution, has a variance that is proportional to its mean. When used on a 'dB relative to average' scale, this means that the standard deviation σ in dB is constant. For the Log-Rayleigh, case it can be shown that $\sigma = 5.7$ dB and we note that the results for CSO/CTB (as seen in Figure 2) terms do not differ appreciably from this value, although at the tail of the distribution CTB peak values are slightly higher than those of the CSO and Log-Rayleigh terms (Figure 2b). In that figure, the modulated case (broken lines) is seen to have higher relative envelope values than the CW case for the same probabilities with a difference of less than half a dB at the level of interest. Although the absolute values for the modulated case are some 2.5 dB lower than the CW case (having peak sync amplitudes), we are showing here the results normalized to average power.

The trends observed in these simulations are fairly consistent with measurement results of a real headend as reported in Reference [4] (see Figures 8 and 9 in that reference), although the difference between the modulated case and the CW case in the measurement results seems to be slightly larger. It is conjectured that because the video sources in that system were received from a satellite feed, as would be the case for many cable systems, some were in fact correlated, as they carry program material that is frame synchronized across various channels[4]. Hence, more of the variations attributable to amplitude modulation were based on even fewer degrees of freedom, increasing the relative statistical dependence among these components.

[4] Many of the services such as the HBO group of channels come from a single uplink facility wherein the practice of video 'house sync' is used. Other examples of groups that are likewise synchronized are the Viacom feeds and the USA Network feeds.

Turning back to the question raised at the outset, tying these statistics to the impact on digital channels is rather straightforward. As can be seen in Figure 2b, both CTB and CSO components have significant likelihood of having peak envelope power fluctuations that exceed their average power levels by more than 12-18 dB. Unfortunately, when such fluctuations occur in a composite distortion term having an *average* level of –47 dBc, levels up to –29 dBc can be experienced. Thus, even in situations in which the prevailing noise floors are rather intuitively low, significant impairments can still be observed. To relate these results to 256 QAM Bit Error Rates (BER) and consequential video impairments we turn next to the temporal characteristics of these composite distortion components.

4.3.2 Time Domain Statistics of Composite Distortions

While we have not simulated the second-order properties of these distortion components, several observations can be made. When high envelope fluctuations of composite distortion terms occur, bursts of bit errors can be generated on the 256 QAM link. Degradations due to bursts that are relatively short can be mitigated in part by the interleaving used on the digital link. Such interleaving is part of the Forward Error Correction (FEC) system used in QAM transmission. Clearly, there would be more severe degradations for burst errors with durations that exceed the interleaver depth capability. Figure 3 shows experimental results that demonstrate that fact for 256 QAM. As can be seen in this figure, substantial reduction in coded error rate is achieved with interleavers that have depths longer than 50-100 microseconds. Improvements start to level off above 200 μs, indicating that there are much fewer burst events that are longer than 200 μs. This observation shows that the characteristic duration of CSO peak envelope fluctuations is on the order of 100 μs. These results appear consistent with other studies on CSO/CTB distortion effects. See for example the similar average durations (60 μs) reported by Germanov [2].

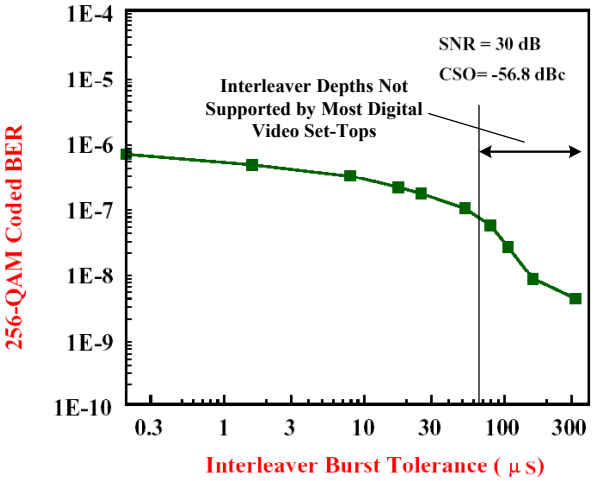

Figure 3. Coded bit error rate of 256 QAM link perturbed by CSO distortion as a function of interleaver burst span. The 256 QAM signal was carried 5.6 dB below the analog carriers, making the CSO average power level shown in the figure -51.2 dBc interference for the QAM channel. Source: Ref. [3].

While both authors in References [2] and [3] report the phenomenal fact of this characteristic duration times, neither suggests a mechanism, a reason or a cause for the observed 100 μs characteristic times. As explained below, these characteristic times are simply related to the correlation times of the individual composite distortion components. These, in turn, are inversely related to the effective bandwidth occupied by such distortion components.

Figure 4 depicts a conceptual rendition of the power spectrum of a composite distortion term produced in a non-coherent frequency plan. Because most of the power of these distortion terms is distributed around frequencies that are a linear combination of the nominal frequencies of the contributing carriers [i.e. $f_1 \pm f_2 \pm f_3$ (for CTB) or $f_1 \pm f_2$ (for CSO)], the

spectral spreading for most of the energy will be on the order of several times the *frequency tolerance* of all transmitters. Some energy due to video modulation in the first (dominant 15.7 kHz horizontal rate) sidebands will widen this somewhat to a power bandwidth on the order of 10 kHz. For such narrow-band processes, the correlation times are approximately inversely proportional to the power bandwidth Δf and for a 10 kHz wide CTB or CSO spectral "clump", one obtains $\tau = 1/\Delta f = 1/10^4 = 100\mu s$ for the characteristic time. Thus, for these narrow-band composite distortion components, the envelope value cannot change appreciably in less than 50-100 μs, thereby giving rise to durations of peaks on that order. Ironically, modern (and more frequency accurate) transmitters, or for that matter, for carrier frequencies produced in a coherent headend, wherein all distortion terms fall on the same frequency, the effective power bandwidth could be substantially smaller (as shown schematically in Figure 4). This will result in longer characteristic times for burst errors associated with composite distortions. Unfortunately, as labeled in Figure 3, most digital video set-tops do not have sufficient interleaver memory to adequately protect against the *most likely* burst durations, as they are limited to a protection depth of 66 μs in the 256 QAM mode[5]. In contrast, that same memory limit provides these set-tops a longer (95μs) interleaver span in the 64 QAM mode, which further enhances the error tolerance of 64 QAM links as compared to 256 QAM.

It is in the context of this CTB/CSO burst vulnerable regime of 256 QAM that we examine the effect of additive noise in the channel. A *C/N* value of 30 dB, a value some would have judged as sufficient for 256 QAM, is shown in Figure 3 to be dramatically inadequate for 256 QAM operation under CSO distortion values that more than meet most MSO's operating standards.

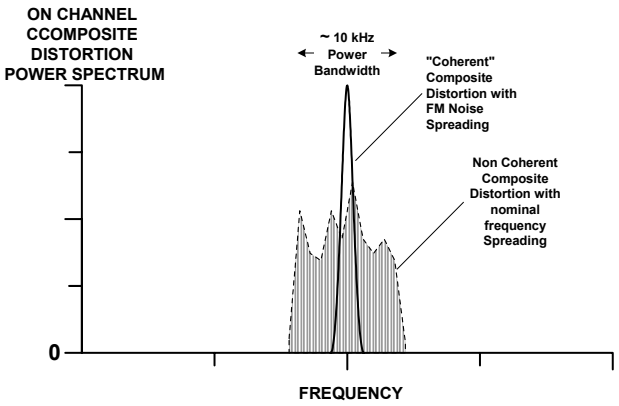

Figure 4. Conceptual rendition of the power spectrum of a composite distortion term produced in a non-coherent frequency plan and that produced in a coherent plan, wherein all distortion terms fall on the same frequency. Because most of the power is distributed around frequencies $f_1 \pm f_2 \pm f_3$ (for CTB) or $f_1 \pm f_2$ (for CSO), the spectral spreading for most of the energy will be on the order of several times the frequency tolerance of all transmitters. Some energy due to video modulation in the first 15.7 kHz (horizontal rate) sidebands will widen this somewhat to a power bandwidth on the order of 10 kHz.

Figure 5 shows measurement results reported in Reference [4] using real set-tops and real head-end live video sources to modulate each channel in the analog tier. Uncoded bit error rates were recorded as a function of total interference and noise power. Note that at target BER values of 10^{-8}, up to an additional 15 dB(!) of Noise+Interference margin is required for 256 QAM over that of 64 QAM. This increment is significantly larger than the 5.6 dB theoretical increment expected in pure random noise channels [17] and is related to the stacking of unfavorable parameters used in 256 QAM as enumerated in Section 5. Consequently, as further elaborated below and in reference to the results shown in Figure 5, this author suggests that under CSO/CTB levels that are within current operational CATV specifications, a 40 dB *C*/(*N*+*I*), corresponding to a 256 QAM BER of 10^{-6}, would *not* provide adequate margin for reliable 256 QAM operation and that rather,

[5] The 66μs protection mode in 256 QAM can be set by selecting I=128,J=1 for the convolutional interleaver.

$C/(N+I)$ values in the range of 43-45 dB (approaching uncoded BER of 10^{-8}) would be required for a Quasi-Error-Free (QEF) 256 QAM operation[6].

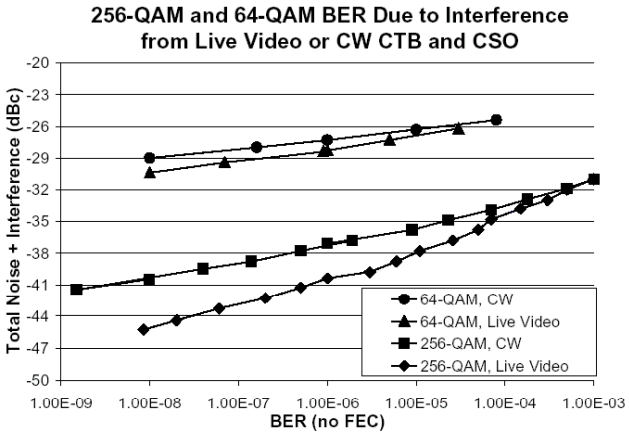

Figure 5. The measured effect of composite distortions on uncoded BER of 256 QAM link as compared with 64 QAM. CTB and CSO distortions were from analog carriers that were either modulated (Live Video) or unmodulated (CW). Note that at target BER values of 10^{-8}, an additional 11 dB of Noise+Interference margin is required for 256 QAM over that of 64 QAM. Source: Ref. [4].

Finally, it should be appreciated that many of the digital 256 QAM channels are likely to be situated well above the 550 MHz boundary and, as such, will be subject to both CTB and CSO. In this case, two distortion contributions should be accounted for. For our purposes below, we shall assume two composite distortion components each at a level of –55 dBc. This corresponds to -49 dBc with respect to the 256 QAM signal, resulting in an average composite distortion level of –46 dBc.

[6] Quasi Error Free (QEF) reception should be distinguished from reception at the impairment Threshold Of Visibility (TOV). The Europeans set the QEF standard for DVB at levels achieving less than one uncorrected error event per hour [18]. In North America, J-83 Annex B defines QEF at less than one uncorrected error event per 15 minutes [21],[22]. The latter event uncorrected error rate corresponds to a BER = 4.0E-11 at the input of the MPEG-2 demultiplexer.

4.3.3 How large can CSO/CTB envelope fluctuations become?

The answer to this question depends on the observation interval. For practical purposes, we shall first present an intuitive approach to this problem, as it will establish better understanding of the reasons for a substantial rethinking of the required margins for reliable 256 QAM operation.

First, we pose the question slightly differently by noting that the problem is essentially that of Level Crossing Rate. Next, we note that according to the discussion above, the envelope of the composite distortion term is essentially uncorrelated with its values separated by more than the characteristic time. Thus, for approximation purposes, we shall make the assumption that values of the envelope at time instances that are more than 300 μs apart are essentially statistically independent. This means that on average, every 300 μs the envelope has an independent ability to achieve any value in accordance with the probability density shown in Figure 2. Stated another way, every 300 μs, we get to make an independent experiment and draw at random a new envelope value with *a-priory* probability shown in Figure 2. If one uses the North American Quasi-Error Free rate as the permissible error event rate, then on average, we have 15 minutes of many 300 μs experiments to encounter one error event. Assuming for simplicity that the average distortion level is at such a level that only the highest excursion causes an uncorrected error, this means that we have $15\times60/(300\times10^{-6}) = 3\cdot10^{6}$ independent experiments of which only one needs to produce the largest envelope value causing an error event. Stated another way, the level crossing probability need only be one in three million (3.33×10^{-7}). By inspecting Figure 2b for CTB and roughly extrapolating down below the 10^{-6} probability density line, one can estimate that by integrating its tail over

the last few dB bins, we would pick up a probability mass of 3.33×10^{-7} for all values above 16 dB. Hence, we thus estimated that the probability that the envelope exceeds the value of 16 dB is 3.33×10^{-7}. This means that the CTB envelope will exceed a level that is 16 dB above its mean at an average rate of once per 15 minutes.

4.3.4 CSO/CTB Relationship to peak amplitudes of multicarrier signals.

Over the years, an intuition seemed to have developed among CATV engineers with respect to the causal relationship of composite distortion fluctuations and excessive amplitude excursions of the composite multicarrier signal. This intuitive view envisions situations in which occurrences of high peak amplitudes of the multicarrier system are the cause of, and are therefore time-coincident with, interference transients associated with excessive distortion components. This view appears to be further supported by observations that a rapid increase in distortion-induced impairment rates are seen when nonlinear devices are driven beyond certain high levels. The intuitive theory often advanced in relation to that observation is that at those high signal levels, the composite amplitudes of the multicarrier signal reaches clipping (saturation) levels which *simultaneously* produces transient distortion products. Many measurements were attributed to such mechanism and many models based on this theory were published and analyzed (see [19] and the extensive reference list in Reference [20]). As we shall se below, peak amplitude fluctuations of CSO or CTB terms produced by *pure parabolic and cubic* nonlinear characteristics can produce sharp degradation effects that are often unnecessarily attributed to the proverbial clipping mechanism at multicarrier signal levels that are significantly lower than actual clipping levels. To that end, simulation results for the Joint Probability Density of the envelope of a multicarrier signal and the envelope of resultant composite distortion components falling out of the analog channel tier (on channel 105), where digital signals might be carried are shown with contour plots in Figure 6. Note that very little correlation exists between the instantaneous levels of distortion terms and the composite signal. It is seen that the highest peak values of CTB (a) or CSO (b) will be encountered even when the composite multicarrier envelope is around its most likely value. Although the CTB plot shows mild correlation at high levels, virtually all occurrences of large peak values for CSO and CTB are found with composite multicarrier amplitudes that are within 2 dB of their average.

In this regard, it is worth noting that an abrupt degradation can result by simply overdriving a *smooth* second-order or third-order nonlinearity. This can readily be seen in Figure 2, where it can be appreciated that at the tail of the density function, where peak values can reach an observable degradation event, there is roughly one order of magnitude increase in occurrence rate for every dB increase of average distortion power. For CTB distortions, this means that if a drive level is just before the Threshold Of Visibility (TOV), overdriving the device by only one more dB, causes CTB to increase by 2 dBc, which corresponds to 100-fold(!) increase in the occurrence rate of visible degradations. At an initial TOV condition of, say, once every 10 seconds, the degradation rate would rise to 10 per second. That dramatic change over a one dB level change would sure look like a "clipping" phenomenon to many folks…but it is not. It is simply the result of *overdriving* the nonlinear device.

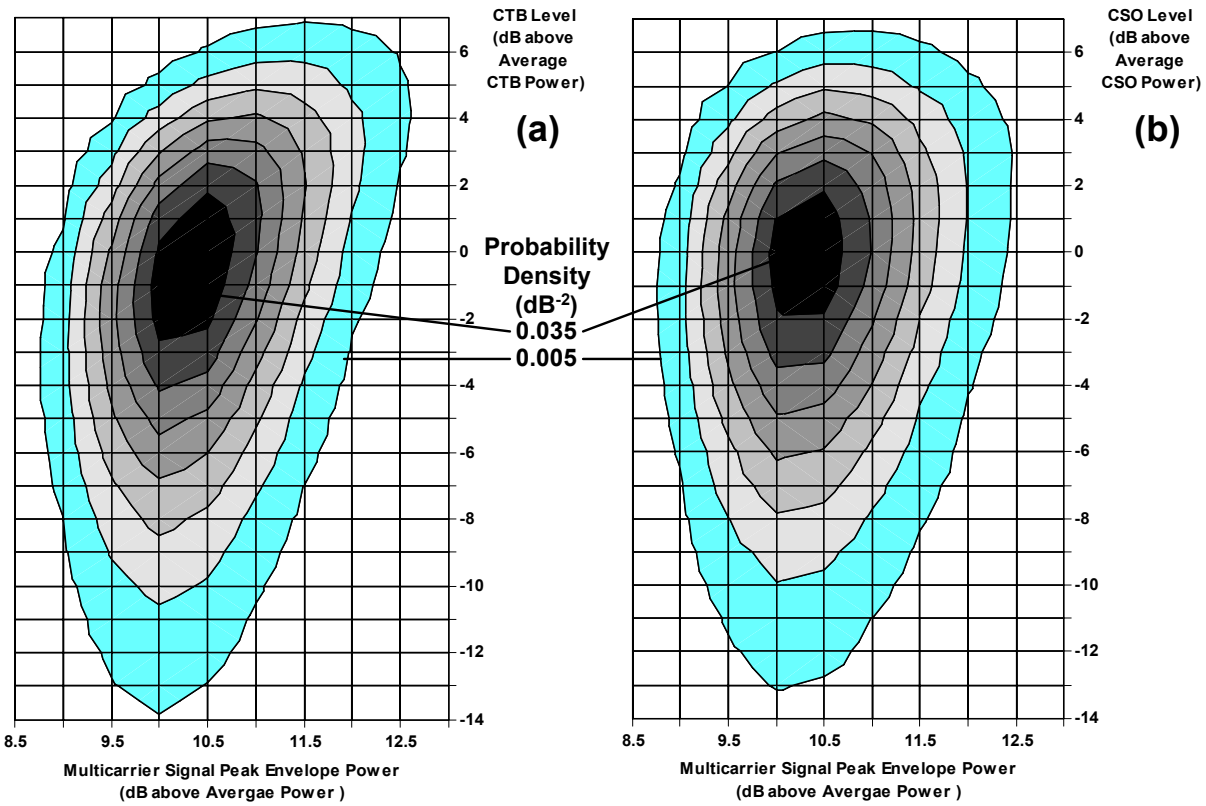

Figure 6. Simulation results for the Joint Probability Density of the envelope of a multicarrier signal with 75 carriers and the envelope of resultant composite distortion components on individual high channels. Note that very little correlation exists between the instantaneous levels of distortion terms and the composite signal. It is seen that the highest peak values of CTB (a) or CSO (b) will be encountered even when the composite multicarrier envelope is around its most likely value. In other words, "clipping" is not the most likely cause of CTB/CSO peak value excursions. Probability density contours are 0.005 per dB^2 apart**.**

In fact, in some devices, clipping values would be far from the lower levels that would otherwise render *smooth* nonlinear devices inoperable due to overdrive. There is no doubt that situations are being encountered wherein clipping is a factor in observed degradations, but as we have seen, "clipping" is not the most likely cause of excessive CTB/CSO peak value excursions. By definition, it is the higher order distortion terms that must be associated with clipping. On this likelihood balance, perhaps a more fitting title for the article in Reference [19] would have been "Don't Get *Overdriven* on the Information Highway"….

5 Moving Forward with 256 QAM

5.1 Where we are

The previous sections illustrated how the challenges associated with operating a reliable 256 QAM service far exceed those associated with the 64 QAM digital services that operators have grown accustomed to. The reasons for the substantial difference in immunity from interference between the two formats can be found by examining their parameters. A summary of relevant factors is shown in Table 1.

Item	64 QAM	256 QAM	Comment on 256 QAM vs. 64 QAM
Constellation Density	8 x 8	16 x 16	
Half Symbol Spacing to RMS Signal (dB)	-16.23	-22.30	6 dB denser
Nearest Symbol Angular Separation (Degrees)	7.7	3.7	Less than half
Symbol Rate (Msps)	5.056941	5.360537	
Channel Data Rate (Mbps)	30.341646	42.884296	
Information bit rate (Mbps)	26.97035	38.8107	44% More Traffic
Overall Channel Utilization Rate	88.89%	90.50%	Due to Coding and Framing Overhead
Excess Bandwidth Roll-off Factor	0.15	0.12	Higher implementation loss with small Roll-off
Interleaver Span Supported by Set-Tops (μsec)	95	66	Due to limited RAM Implementations

Table 1. Comparison of various transmission parameters of 64 QAM and 256 QAM in the North American standard. See [21],[22].

These factors and others are addressed below:

(a) *Symbol constellation density* is two times that of 64 QAM in each dimension. This means that relative to the signal level, decision regions in the 256 QAM signal space occupy an area that is one quarter of that of 64 QAM.

(b) *Burst error interleaver depth* is limited in most set tops to 66 μs in 256 QAM mode as opposed to 95 μs in 64 QAM mode.

(c) *Coding Gain* is lower for the 256 QAM format which has a trellis code rate of 19/20, dedicating one bit out of 20 for forward error correction versus one out of 15 bits used in the trellis code for 64 QAM.

(d) *Spectral Roll-Off Factor* of 0.12 for 256 QAM (vs. 0.15 in 64 QAM) further reduces demodulator "eye opening" margin, which increases demodulation implementation losses.

(e) *Reduced Immunity to CSO and CTB* distortion products (as discussed above).

(f) *Higher Susceptibility to phase noise* [3] and 'microphonics'.

(g) *Increased Tracking Time of the Adaptive Equalizer.* Due the finer constellation of 256 QAM, channel adaptation time to sufficiently low symbol interference can take longer than in 64 QAM especially if the demodulator employs a smaller step size for the coefficient updates in 256 QAM. A longer Equalizer convergence time can degrade its ability to effectively track and null out a discrete interferer with level and spectral fluctuations at rates that exceed the equalizer convergence time constant[7].

These factors are the realities that cannot be changed by operators. We turn next to steps that can be taken to improve the viability of 256 QAM in more and more systems.

[7] Convergence times of the order of 2,000-10,000 symbols are not uncommon. This means that for a 5 Msps QAM signal, fluctuations faster than 1 kHz would not be tracked well. Unfortunately, as seen above, the characteristic times of the CSO/CTB fluctuations are an order of magnitude faster. However, in the CW mode, these CSO and CTB components have a narrower spectral spreading and consequently might be better tracked by the equalizer. This may explain the data in Figure 5 showing the significant improved immunity of demodulators subject to CW CSO/CTB interference as compared to modulated CSO/CTB interference.

5.2 Where we need to go

In order to successfully employ 256 QAM services we would be well advised to consider the following mitigation measures and improved practices:

5.2.1 Control and improve CSO/CTB levels

This is an obvious item, but operators should consider reviewing their plant distortion budgets. A –53 dBc at the subscriber tap would not leave any margin for subscriber equipment degradations. In addition, CSO/CTB specifications of subscriber tuner distortion warrant further scrutiny. Several cable modem tuner suppliers offer specifications for CSO and CTB that are in the –50 dBc range. As explained above, if such average levels of distortions are encountered (-44 dBc for the digital signal), 256 QAM operation would be unreliable[8]

5.2.2 Employ judicious choice of channel frequency offsets

As described above, CSO and CTB components have most of their energy clustered in a spectral region spanning no more than 30 kHz. The most powerful CTB component consists of a combination of terms with frequencies $2f_1$-f_2, which falls on what would be the NTSC visual carrier frequency for that channel. Thus, it is narrowly concentrated 1.25 MHz above the channel edge. In a paper presented to the Joint EIA-NCTA Engineering Committee a decade ago [24], this author suggested the use of a frequency offset scheme that can virtually eliminate interference from these CTB components by moving the digital channels up by 1.25 MHz with respect to the analog channel boundaries. This way, the CTB components are situated at the edge (in between) of the digital channels where there is considerable rejection by the receiver's SAW filter and the digital matched Nyquist filter. As discussed in [24], this relative offset is also optimal for minimizing third-order noise distortion emanating from the digital channels and falling on the analog channels.

Unfortunately, not all distortion terms are being rejected that way. Second order distortion terms of the $f_1 + f_2$ class situated 2.5 MHz above the channel edge are not rejected and since their level may increase at higher frequencies in the channel lineup (accompanied by a fortuitist decrease in the levels of CTB terms), one may wish to institute a new offset of an *additional* 1.25 MHz for digital channels above a certain cross-over frequency, where CTB levels are lower than CSO levels. Thus, proper channel offsets becomes a balancing act, since one cannot avoid both the CSO and CTB terms simultaneously.

5.2.3 Maintain head-end transmitter aggregate noise power at low values.

In Reference [1], this author shows the significant impact of noise aggregation from many transmitter sources at the headend and hubs. It is shown that under currently prevailing headend and HFC signal transport practices, mass deployment of certain classes of QAM transmitters and upconverters used (or proposed to be used) for VOD, may not scale well because of excessive noise accumulation from adjacent channel modulated distortion terms as well as from broadband noise. It is further shown in Reference [1] that as operators expand and carry 50 digital channels on their downstream lineup, the use of lower performance QAM

[8] For 256 QAM, the cable modem multicarrier loading test in the DOCSIS ATP [23] permits a test under which the total power of 30 dBmV is distributed across 5 carriers (one signal of interest, four other) not on image or adjacent channels. However, such test does not guarantee that any of the intermodulation components fall on the channel of interest. Furthermore, CSO and CTB from only 4 carriers produce much lower peak envelope power fluctuations than 80-channel source having the same total power.

transmitters can result in a 2.4 dB C/(N+I) loss at the subscriber tap compared to the levels that can be realized with transmitters that meet the DOCSIS downstream QAM transmission requirements as provided in Table 6-15 of its Radio Frequency Interface Specification [25].

5.2.4 Secure next generation transmitters and set-tops with specific improvements

From the deficiency list compiled in Section 5.1 above, we turn to two items:

5.2.4.1 Increased interleaver depth

As seen in our discussion above and as presented in some of the test results, the interleaver depth supported by most set-tops today is decidedly inadequate for the type of channels found in CATV. A further concern is the fact that even some transmitters are incapable of operating at the full depths provided in the standard. Figure 3 shows that an interleaver depth of at least 300 μs would be required to handle CSO and CTB transients. Table 2 shows the various depth options available under J-83 Annex B. It becomes obvious that the earlier one starts to deploy full depth interleaving ,the better. In any event, there is no reason why operators should continue to invest in transmitters that are not fully compliant with all the modes in Table 2.

I **(# of taps)**	***J*** **(increment)**	**Burst protection 64-QAM/256-QAM**	**Latency 64-QAM/256-QAM**	**Comments**
8	16	5.9 μs /4.1 μs	0.22 ms/0.15 ms	DOCSIS Requirement
16	8	12 μs /8.2 μs	0.48 ms/0.33 ms	
32	4	24 μs /16 μs	0.98 ms/0.68 ms	
64	2	47 μs /33 μs	2.0 ms/1.4 ms	
128	1	95 μs /66 μs	4.0 ms/2.8 ms	
128	2	190 μs /132 μs	8.0 ms/5.6 ms	Not supported by most digital video set-tops
128	3	285 μs /198 μs	12 ms/8.4 ms	
128	4	379 μs /264 μs	16 ms/11 ms	
128	5	474 μs /330 μs	20 ms/14 ms	
128	6	569 μs /396 μs	24 ms/17 ms	
128	7	664 μs /462 μs	28 ms/19 ms	
128	8	759 μs /528 μs	32 ms/22 ms	

Table 2. Interleaver Depth Settings available in J-83 Annex B. It is argued that the use of the maximum length associated with (I,J) = (128,8) would be a highly desirable upgrade for new transmitters and set-tops.

5.2.4.2 Improved Adaptive Equalizers

A particularly important feature of adaptive equalization systems employed in demodulators is their ability not only to equalize the channel frequency response by minimizing Inter-Symbol Interference (ISI), but also "equalizing" out interference signals. In the presence of discrete interference signals, many equalizer systems are able to automatically converge to a state that forms a sharp notch at the frequency of the interferer. The degree of rejection and the speed at which these equalizers converge becomes a key attribute of the demodulator. There is no doubt that demodulator chip makers are now

looking at improved equalization techniques with a particular goal of improving the narrow-band rejection capability. The author envisions industry efforts to better characterize and standardize CSO/CTB rejection capability of demodulators so that these attributes become part of a qualification or certification process.

6 Summary and Conclusions

There is reason to review and go over a substantial rethinking of the required margins for reliable 256 QAM operations. It is argued that composite distortion terms having envelope peaks that can reach up to 16 dB above their average level leave very little room for further noise degradations at *any* level of the signal distribution. First-order statistics for CSO and CTB envelopes were simulated and specific degradations due various factors including shorter interleaver spans were analyzed. Finally various mitigation steps have been recommended in order to enable more successful rollout of 256 QAM.

7 Acknowledgement

The author wishes to thank Dr. Andre Basovich of Broadband Innovations, Inc. who programmed the simulations and ran them over many days.

8 References

1. Ron D. Katznelson, "Delivering on the 256 QAM Promise. - Adopting Aggregate Degradation Measures for QAM transmitters". Submitted to *Cable-Tec Expo® Proceedings*, SCTE, (June 2002).

2. Vitaly Germanov, "The Impact of CSO/CTB Distortion on BER Characteristics by Hybrid Multichannel Analog/QAM Transmission Systems". *IEEE Transactions on Broadcasting* **Vol 45**. No. 3. pp. 348-352, (September 1999).

3. Shlomo Ovadia, "The Effect of Interleaver Depth and QAM Channel Frequency Offset on the Performance of Multichannel AM-VSB/256-QAM Video Lightwave Transmission Systems". *NCTA Technical Papers*, (1998).

4. Dean Stoneback, Robert Howald, Timothy Brophy and Oleh Sniezko, "Distortion Beat Characterization and the Impact on QAM BER Performance". *NCTA Technical Papers*, (1999) (Downloadable at http://www.gi.com/whitepaper/CTBNCTA99Final.pdf).

5. Robert Howald, "QAM Bulks Up Once Again: Modulation to the Power of Ten". Submitted to *Cable-Tec Expo® Proceedings*, SCTE, (2002).

6. *Digital Cable Network Interface Standard*. SCTE 40 2001 (Formerly DVS 313), (2001).

7. Ken Simons, "A mathematical Analysis of Distortion as it Occurs in CATV Amplifiers" Ch. V in *Technical Handbook for CATV Systems*. General Instrument, 3rd Edition (1968).

8. Ron D. Katznelson, "Optimal Signal Synthesis for Distortion Canceling Multicarrier Systems". U.S. Patent No. 5,125,100, (June 23, 1992).

9. W. R. Bennett, "Cross-Modulation Requirements on Multichannel Amplifiers Below Overload", *Bell System Technical Journal*, **Vol. 19**, pp. 587-605, (1940).

10. Matrix Technical Notes MTN-108, "Some Notes On Composite Second and Third Order Intermodulation Distortions", (Dec15, 1998). (downloadable at http://www.matrixtest.com/Literat/mtn108.htm)

11. Ron D. Katznelson, "Higher Order Statistics of Composite Distortion Components in Multicarrier Systems". In preparation (2002).

12. J. Dugundji, "Envelopes and Pre-Envelopes of Real Waveforms", *IRE Transactions on Information Theory*, **Vol. IT-4**, pp. 53-57, March (1958).

13. P. Mazur and E. Montroll, "Poincare Cycles, Ergodicity and Irreversibility in Assemblies of Coupled Harmonic Oscillators". *Journal of Mathematical Physics*, **Vol. 1**. No. 1. pp. 70-84. (1960). See Appendix III.

14. J. Davidse, "NTSC colour-television signals – evaluation of measurements", *Electronic & Radio Engineer*, pp. 416-419, November (1959).

15. Darryl Schick, "Characterization of Peak Factor Effects in HFC Systems Using Phase Controlled Carriers", *NCTA Technical Papers*. pp. 44-47. (1996).

16. A. Papoulis, *Probability, Random Variables and Stochastic Processes*, McGraw-Hill (1965).

17. Dojun Rhee and Robert H. Morelos-Zaragoza. "Error Performance Analysis of a Concatenated Coding Scheme with 64/256-QAM Trellis Coded Modulation for the North American Cable Modem Standard, *Proceedings of the 1998 IEEE International Symposium on Information Theory (ISIT '98*), p. 61, MIT, Cambridge, August 17-21, (1998).

18. European Telecommunications Standards Institute, "Digital Video Broadcasting (DVB) Framing Structure, Channel Coding and Modulation for Digital Terrestrial Television" *EN 300 744* (January 2001).

19. D. Raskin, D. Stoneback, J. Chrostowski and R. Menna, "Don't Get Clipped on the Information Highway".). *NCTA Technical Papers*. pp. 294-301. (1996).

20. Qun Shi and Robert S. Burroughs, "Hybrid Multichannel Analog/Digital CATV Transmission via Fiber Optic Link: Performance Limits and Trade-Offs", *NCTA Technical Papers*. pp. 182-193. (1994).

21. American National Standard, *Digital Video Transmission Standard for Cable Television,* ANSI/SCTE 07 2000 (Formerly SCTE DVS 031). (Downloadable at http://www.scte.org/standards/pdf/standardsavail/ANSI-SCTE%2007%202000.pdf).

22. ITU-T Recommendation J.83 Annex B. "*Digital Multi-Programme Systems for Television Sound and Data Services for Cable Distribution*". (April 1997).

23. Section 2.1.7 of "DOCSIS Acceptance Test Plan", TP-RFI-ATPv1.1-I02-010919. CableLabs, September 19, (2001). (Downloadable at http://www.cablemodem.com/specifications.html).

24. Ron D. Katznelson, "Common Architectures for digital and analog receivers" Presented at the EIA/NCTA Joint Engineering Committee. Washington D.C., Fall (1992).

25. "DOCSIS Radio Frequency Interface Specification", SP-RFIv2.0-I01-11231. December 31, (2001). (Downloadable at http://www.cablemodem.com/specifications.html).

***

Author contact:
Dr. Ron D. Katznelson, CTO
Broadband Innovations, Inc.,
3550 General Atomics Ct. Bldg. 15
San Diego CA, 92121

ron@broadbandinnovations.com
(858) 395-1440 Mobile
(858) 713-8505 Office